Insulating states of a broken-gap two-dimensional electron-hole system

K. Takashina, R. J. Nicholas, B. Kardynal, and N. J. Mason

Department of Physics, University of Oxford, Clarendon Laboratory, Parks Road, Oxford OX1 3PU, United Kingdom

D. K. Maude

GHMFL, MPI-FKF/CNRS, Boîte Postale 166, F-38042 Grenoble Cedex 9, France

J. C. Portal

GHMFL, MPI-FKF/CNRS, Boîte Postale 166, F-38042 Grenoble Cedex 9, France
INSA, 135 Avenue de Rangueil, 31077 Toulouse Cedex 4, France
and Institut Universitaire de France, Toulouse, France

It has recently been found that an InAs/GaSb based electron-hole system exhibits insulating behavior with unusual properties when the numbers of occupied electron and hole Landau levels are equal [R. J. Nicholas, K. Takashina, M. Lakrimi, B. Kardynal, S. Khym, N. J. Mason, D. M. Symons, D. K. Maude, and J. C. Portal, Phys. Rev. Lett. **85**, 2364 (2000)]. In this insulating state, the Hall resistance becomes symmetric (even) under field reversal $[R_{xy}(B) = R_{xy}(-B)]$, and both the Hall and longitudinal resistances display reproducible fluctuations. In this paper we present experimental studies of the geometry dependence of this phenomenon. In particular, we show conclusively that the conduction responsible for the reproducible fluctuations and the symmetric Hall resistance occur due to the presence of the mesa edge. Further investigations of the edge conductance are presented. We show that as a function of magnetic field, the edge conduction shows a qualitatively opposite behavior to the conductivity in the sample interior. This is confirmed through measurements with an in-plane component of magnetic field. Also, the size of the conductance fluctuations is found to have a monotonic relationship with the absolute value of the conductance. A model based on counterpropagating edge channels is presented which qualitatively accounts for the observed behavior.

I. INTRODUCTION

In this paper we report and discuss observations of an insulating state of an InAs/GaSb based two-dimensional electron-hole system in high magnetic field. InAs/GaSb is a broken-gap system with the ability to possess both electrons n_e and holes n_h in equilibrium through intrinsic charge transfer without the use of doping or the application of an electrical bias.[2–5] The first observation of quantum Hall plateaus in an InAs/GaSb based electron-hole system made by Mendez *et al.*[6] found that plateaus were formed at quantum numbers corresponding to the difference in the occupancies of the electron and hole Landau levels. When the net carrier concentration $(n_{net} = n_e - n_h)$ is small (e.g., $n_{net} \sim 2 \times 10^{15}$ m^{-2} for n_e of order 7×10^{15} m^{-2}), a special condition can be achieved in magnetic field due to conductance quantization where there are effectively equal numbers of occupied electron and hole Landau levels such that $\nu_e - \nu_h = 0$, while ν_e and ν_h are both finite. Such a state was first observed by Daly *et al.*[7] who found that the resistivity defined by

$$\rho_{xy} = \tfrac{1}{2}[R_{xy}(B) - R_{xy}(-B)] \tag{1}$$

became vanishingly small, while the longitudinal resistivity ρ_{xx} became large. This was interpreted as being due to both diagonal and Hall conductivities σ_{xx} and σ_{xy} tending to zero due to the electrons and holes contributing quantized Hall conductivities in opposite directions but equal in magnitude.

It has recently been found[1] that the symmetric part of the measured Hall resistance R_H^S defined by

$$R_H^S = \tfrac{1}{2}[R_{xy}(B) + R_{xy}(-B)] \tag{2}$$

displays properties which cannot be accounted for as being due to a geometric admixing of the diagonal resistivity ρ_{xx}. R_H^S becomes too large, bears no simple relationship to the longitudinal resistance R_{xx}, and displays reproducible fluctuations. In the initial paper reporting the phenomenon,[1] it was proposed that the edge states[8] in this insulating state could be such that the current distribution is highly distorted.

In this paper, we present geometry dependence measurements which conclusively show that the conduction leading to the reproducible fluctuations and the symmetric Hall resistance occur due to the presence of the mesa edge. Further experimental investigations into the edge conduction reveal that the size of the fluctuations has a monotonic relationship with the magnitude of the edge conductance, and that the edge conductance has an opposite behavior to the conduction in the sample interior with magnetic field. A simple model is proposed to qualitatively account for the behavior observed. The model is based on counterpropagating edge channels where the electron and hole layers contribute channels conducting in opposite directions.

II. SAMPLES AND OVERALL BEHAVIOR

The samples studied consisted of a single layer of InAs in between layers of GaSb close to the sample surface. This
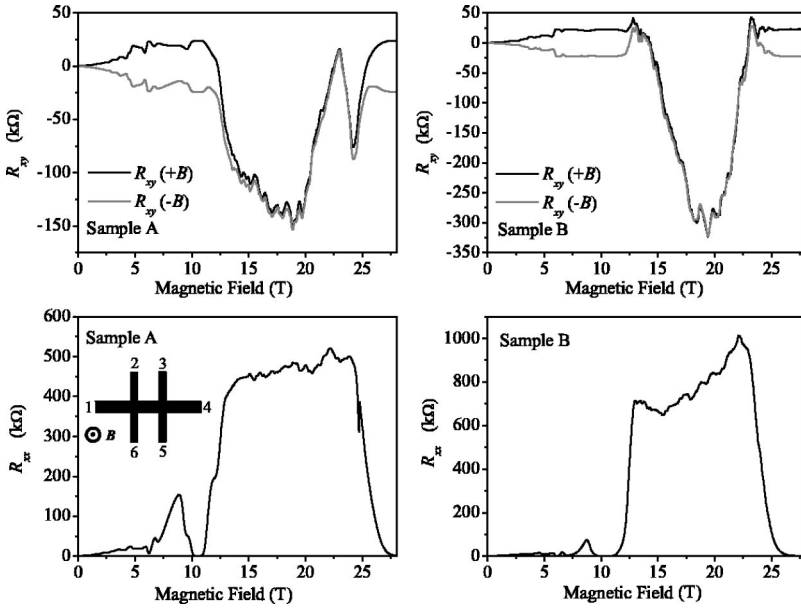
FIG. 1. Magnetotransport data from Hall bars. An inset shows a schematic diagram of a Hall bar. The upper graphs show the Hall resistances $R_{xy} = V_{3,5}/I_{1,4}$. The black lines show data taken with the magnetic field in one direction, while the gray lines show data taken with the magnetic field pointing in the opposite direction. The lower graphs show the longitudinal resistances $R_{xx} = V_{6,5}/I_{1,4}$. The graphs in the left (right) column show data from sample A (B).

system has a broken-gap lineup with the conduction-band edge of InAs 150 meV below the valence-band edge of GaSb.[2–5] The structures were grown by metal organic vapor phase epitaxy[9,10] and have relatively low levels of impurities so that the majority of the charge carriers are created by intrinsic charge transfer. They are grown on GaAs substrates with a 2-μm-thick buffer layer of GaSb to achieve lattice relaxation and this is followed by 30 nm of InAs and 120 nm of GaSb.

In this paper, we explicitly present data taken from samples fabricated from two wafers. Figure 1 shows magnetotransport data taken from Hall bars fabricated from these wafers. These are labeled samples A (OX3616) and B (OX3733). The Hall bars were rectangular and macroscopic in size ($W = 0.5$ mm), with a longitudinal length $L = 1$ mm between voltage probes which were orthogonal to the bar with width of order 100 μm. A dilution refrigerator and a 20-MW resistive magnet was used. A standard AC lock-in technique was used with a 20 nA driving current at a frequency of order 1.7 Hz, ensuring that the out-of-phase components of the signals remained very small. Data from samples A and B are typical of samples studied.[1]

At 10.5 and 28 T, there are quantum Hall plateaus corresponding to an effective occupancy of one.[6] At these fields and below 7 T, the Hall resistance is almost completely antisymmetric (odd) under field reversal: $R_{xy}(B) = -R_{xy}(-B)$. The symmetric part, which might be attributed to the geometric misalignment of the Hall probes, is less than 1% of the longitudinal resistivity. Between 12.5 and 25 T, however, where the quantized occupancies ν_e and ν_h are expected to be equal ($\nu_e - \nu_h = 2 - 2 = 0$), the Hall resistance becomes almost completely symmetric under field reversal. The value of the symmetric Hall resistance is more than 50% of the resistivity. In the same field range, the longitudinal resistance is large, but does not have any obvious functional relationship with the Hall resistance. This rules out the possibility of a simple geometrical admixing of the resistivity as the origin of the symmetric Hall resistance. The usual sym-

metry associated with the Hall resistance[11] is not satisfied. The graphs also show reproducible fluctuations in both the Hall resistance and the longitudinal resistance. These are both symmetric under field reversal. One might enquire whether this peculiar behavior arises through what is commonly termed ''bad contacts.'' We argue, however, that the edges of these samples are fundamentally different to those found in normal single-carrier-type systems, and that the edges dominate the measurements of the insulating state in the Hall bar geometry. In this geometry, the bulk of the system cannot be probed and hence ''contacted'' in the normal way. This is a fundamental property of the system rather than the result of an underdeveloped annealing technology, as is shown by the reappearance of normal behavior above 26 T, and two-terminal measurements we will present in the following section. We have observed this behavior with symmetric Hall resistance with reproducible fluctuations on samples fabricated from 13 different wafers, using different contacting and lithographic techniques.

III. CORBINO DISK

We have studied Corbino disks and Hall bars fabricated from samples A and B. In this section, we show that in the insulating state, the Corbino disk becomes many orders of magnitude more insulating than the Hall bar. We also present temperature dependence measurements.

A. Basic behavior

The Corbino disk was measured using a two-terminal constant voltage technique. Figure 2 shows the conductivity as a function of magnetic field for sample A with an excitation voltage of 10 mV. It also shows the conductivity, as calculated from R_{xx} and R_{xy} as measured from a Hall bar using standard tensor relations.

A distinct minimum can be seen at 10.5 T for both sets of data corresponding to a quantized Hall state. A similar mini-
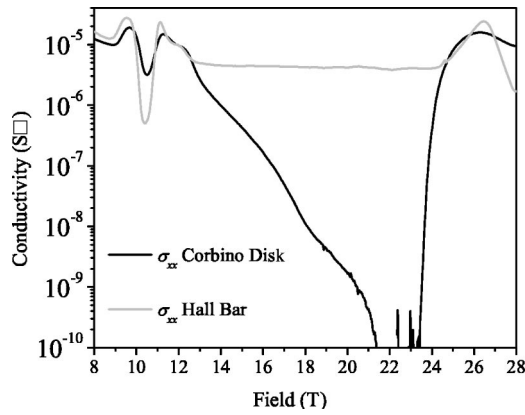
FIG. 2. Conductivity extracted from the Corbino disk and the Hall bar at 100 mK. The Corbino disk was measured with an excitation voltage of 10 mV, and the Hall bar with an excitation current of 20 nA. The conductivity of the Hall bar was calculated applying the standard tensor relations to the measured Hall and longitudinal resistances.

mum can be seen at 28 T. The Hall bar shows deeper minima compared with the Corbino disk due to the large excitation voltage used to measure the Corbino disk.[12] In contrast, in the field range 13–24 T corresponding to the insulating state, the Corbino disk shows values of conductivity that are many orders of magnitude smaller compared with the Hall bar values. In the field range where we expect the Fermi energy to lie within extended states, the agreement between the two measurements is reasonable.

B. Voltage dependence

In order to test that this discrepancy is not due to contacting problems, we have varied the current through the Hall bar and found that the longitudinal resistance we measure has Ohmic voltage dependence over many orders of magnitude, while the Corbino disks show extremely nonlinear behavior. As a more explicit test, we have fabricated a two-terminal device and a Corbino disk from sample B, using identical contacting procedures and measured their current-voltage characteristics using identical experimental configurations.

Figure 3 shows the current passed by a two-terminal bar (triangles) and a Corbino disk (squares) as a function of the applied voltage using identical experimental settings. The data for the two-terminal bar has a gradient of one on the log-log plot. The bar therefore shows Ohmic behavior, while the Corbino disk shows strongly non-Ohmic insulating behavior.

C. Temperature dependence

We return to sample A, and describe its temperature dependence. The two samples of differing geometry were measured simultaneously.

Figure 4 shows data at different temperatures. At 900 mK, the Hall bar shows a relatively smooth variation of resistance with magnetic field. As the temperature is lowered, the resistance increases, but then saturates. The saturation is accom-
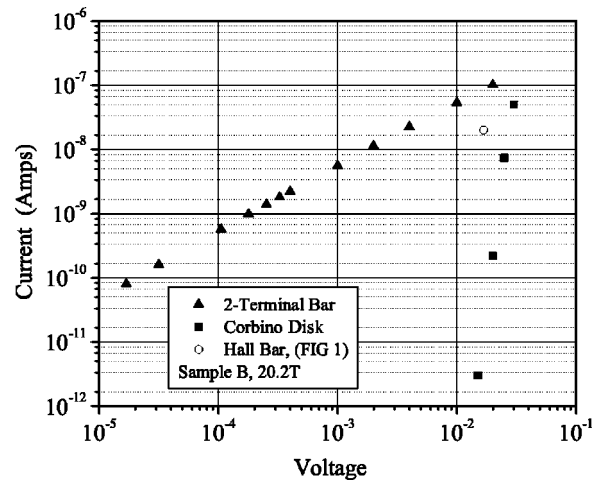

FIG. 3. Current-voltage characteristics of a two-terminal bar ($L = 800 \ \mu$m, $W = 200 \ \mu$m) and a Corbino disk fabricated from sample B at 20.2 T and 50 mK. $V_{6,5}(I_{1,4})$ of the Hall bar whose data is shown in Fig. 1 is indicated for comparison.

panied by the onset of reproducible fluctuations. The Corbino disk however shows insulating behavior down to the lowest temperature where the conductivity continues to decrease with falling temperature.

Figure 5 shows the temperature dependence of $1/R_{xx}$ of the Hall bar. As the temperature decreases, it saturates. The behavior is consistent with the conductance being a sum of a temperature-independent contribution, and a strongly temperature-dependent one due to the conductivity σ_{xx} in the
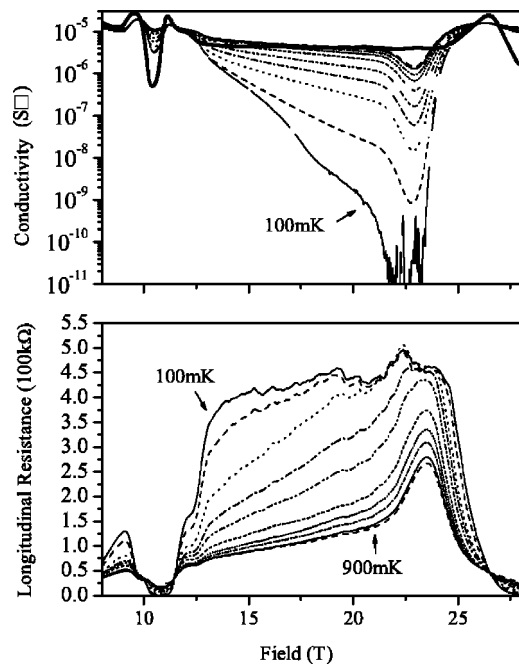

FIG. 4. The conductivity measured from the Corbino disk with an excitation voltage of 10 mV at various temperatures between 100 and 900 mK in steps of around 90 mK. The thick solid line is the data from the Hall bar as described in the preceding section. The lower graph shows the longitudinal resistance measured from a Hall bar.
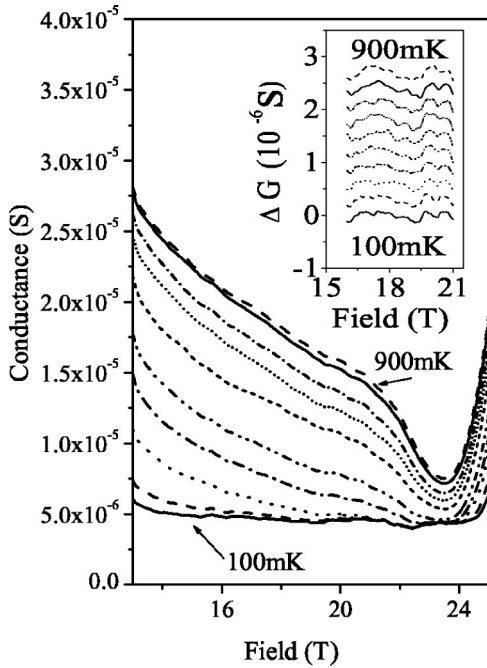
FIG. 5. The conductance as calculated by $1/R_{xx}$ where R_{xx} is measured from the Hall bar as a function of temperature in steps of about 90 mK. The inset shows the fluctuating part of the conductance for the same range of temperature.

sample interior. We attribute the temperature-independent part to the mesa edges. All samples we have measured where the contacts are connected by the mesa edge show this behavior. The inset shows the fluctuating part of this conductance, showing that the scale of the magnetoconductance fluctuations is not strongly temperature dependent between 100 and 900 mK.

D. Discussion

We have shown that at low temperature, the interior of the sample becomes extremely insulating, while the behavior of the Hall bar is dominated by the contribution due to the mesa edges. Samples where the contacts are connected by mesa edges show Ohmic voltage dependence, and the mesa edge contribution to the conductance has very weak temperature dependence.

However, quantitative analysis on this data is difficult. There are two main reasons. First, finite conductance of the Corbino disk can only be measured with large excitation voltages where the conductivity is strongly dependent on the excitation voltage. Second, we will find in the following section that the edge conduction is highly inhomogeneous over macroscopic length scales so that the conductance of the two sides of the Hall bar may be rather different. This would then lead to different current flowing through the two sides of the bar, which places a large uncertainty in the values of the longitudinal "resistance" obtained from V_{xx}/I_{total}. In order to circumvent the latter problem, we have studied two-terminal bars, where the total conductance *must* be given by the sum of the conductance of the two individual edges.
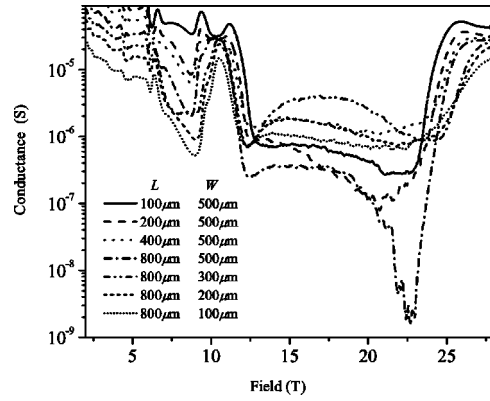

FIG. 6. A graph showing the conductance of two-terminal devices against magnetic field at 100 mK. The different lines correspond to samples with different lengths and widths.

IV. LENGTH, WIDTH, AND IN-PLANE FIELD

Two-terminal bars with different lengths L and widths W, and a Corbino disk were fabricated from sample B. We will first describe the general behavior as a function of sample size. We will then present data where we have applied an in-plane magnetic field. Section IV B will focus on the size of the magnetoconductance fluctuations.

A. Dependence on length and width: Sample-to-sample variations

Figure 6 shows the conductance of two-terminal bars with length and width varied between 100 and 800 μm and 100 and 500 μm, respectively, made from sample B. We have confirmed that they display the expected systematic behavior at values of field outside of the insulating state. In the insulating state however, the sample-to-sample variation is greater than any underlying systematic trend.

Figure 7 shows the conductance of two-terminal devices at three illustrative values of magnetic field as a function of
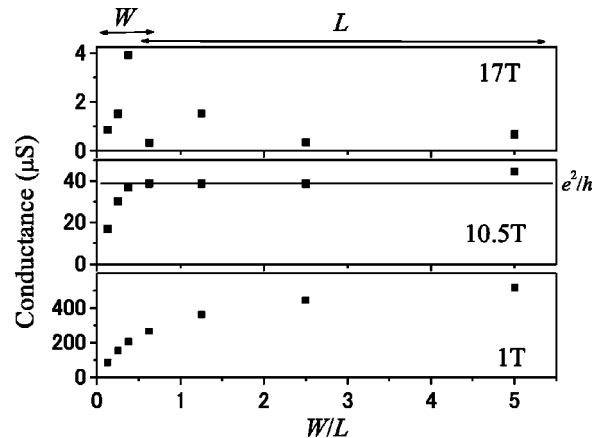

FIG. 7. Plots of the conductance of two-terminal devices as a function of the width-to-length ratio W/L at 17 T (top), 10.5 T (middle), and 1 T (bottom) at 100 mK. The four points of lowest W/L are from samples with width between 100 and 500 μm with length fixed at 800 μm while the four points of largest W/L have length between 100 and 800 μm with width fixed at 500 μm.
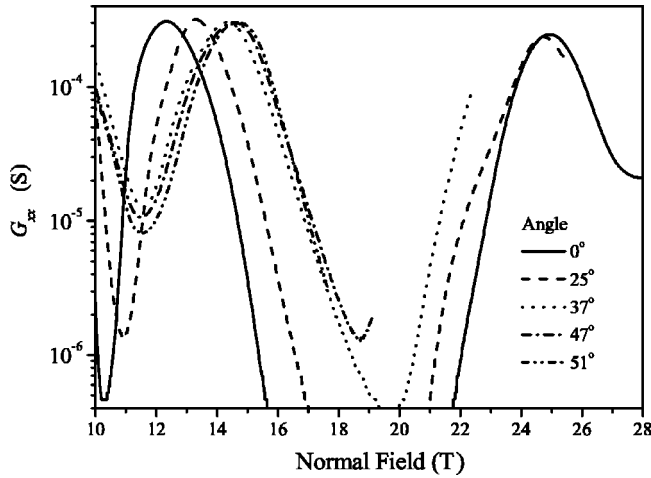
FIG. 8. The conductance of the Corbino disk with an average circumference of 4.08 mm with a difference in radii of 0.2 mm at various angles to the magnetic field at 100 mK. It is plotted as a function of field normal to the sample plane.
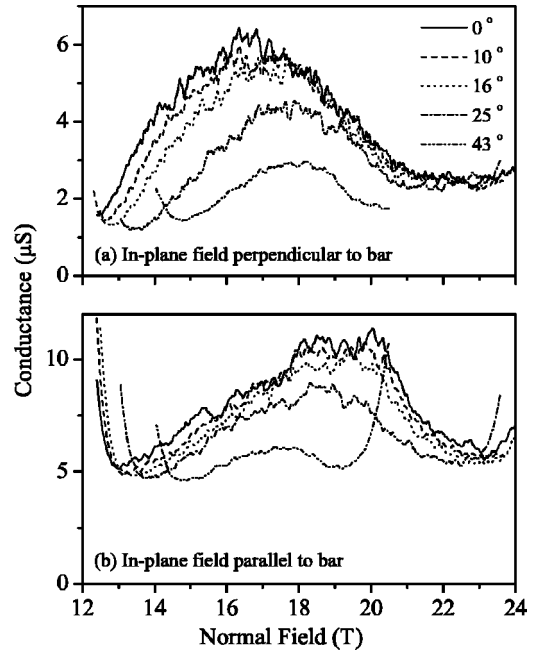

FIG. 9. The conductance of two-terminal bars in tilted magnetic field, as a function of the normal field. (a) The in-plane field is perpendicular to the bar. (b) The in-plane field is parallel to the bar.

the width-to-length ratio. The system shows three different types of behavior. First, at very low field, the behavior is classical. At zero magnetic field, the behavior is completely Ohmic where the contact resistance scales as $1/W$ and the semiconductor conductance scales linearly with W/L. With small magnetic field such as 1 T, the resistance of the bar becomes an admixture of the Hall resistance and the longitudinal resistance. Second, in the more "conventional" compensated quantum Hall regime, e.g., at 10.5 T, the system also shows systematic behavior where for sufficiently long and wide samples, the conductance is given by the quantized value e^2/h. Deviations from this are related to the breakdown of the quantum Hall effect[12] where the behavior is strongly dependent on size and the magnitude of the excitation voltage used. Third, in the insulating regime, the conductance variation from sample to sample is greater than any underlying trend due to changing the width between 100 and 500 μm or the length between 100 and 800 μm.

The strong random variation between the samples suggests a one-dimensional nature of the charge transport. In transport in higher dimensions, the effect of disorder is relatively weak as rare regions of high resistivity can be circumvented by the current. In one dimension, however, the current does not have any degrees of freedom in order to circumvent these regions of high resistivity, and the resistance of the total wire becomes strongly affected by them.

There is however a broad trend with magnetic field followed by all of the samples. All but the narrowest bar show minima in conductance at around 12.5 and 21 T, just after entering and before exiting the insulating state. This suggests that the behavior of the absolute magnitude of the conductance is influenced by factors common to all the samples such as the energies of the Landau levels contributing to the edge states.

We have confirmed this by making measurements with an in-plane component of magnetic field which enhances the spin splitting thereby changing the arrangement in energy of the spin-split Landau levels. Figures 8 and 9 show data from

these measurements. Figure 8 shows data from a Corbino disk while Fig. 9 shows the conductance of two-terminal bars. Two separate bars were measured, one with the in-plane field parallel to the mesa edge, and the other with the in-plane field perpendicular to the mesa edge. We have not seen any conclusive differences due to the difference in the direction of the in-plane field.

As the in-plane field is increased, the conductance of both the two-terminal bars decreases somewhat. In contrast, the conductance of the Corbino disk increases, at some fields by orders of magnitude. The two-terminal bars show an opposite trend to the Corbino disk confirming that the conduction at the mesa edge is not limited due to a leakage through interior states.

Another aspect to note is that the fluctuations change completely between one angle and the next. For instance, between 0° and 10°, the smoothly varying conductance in the background has not changed very much. However, the small scale fluctuations are completely different. This strongly suggests that the origin of the fluctuating behavior is due to interference effects between electrons traveling through different paths[13] as is the case for universal conductance fluctuations.[14]

B. Conductance fluctuations

Examining the fluctuations visible in the data presented in Fig. 9 (and Fig. 6) we see that the size of the conductance fluctuations decreases when the conductance itself decreases. In order to study the size of the fluctuations, we have subtracted a smooth background from the conductance for each dataset $G(B)$. The smooth background was generated by fitting a ninth-order polynomial through the data. This is illustrated in the inset of Fig. 10.
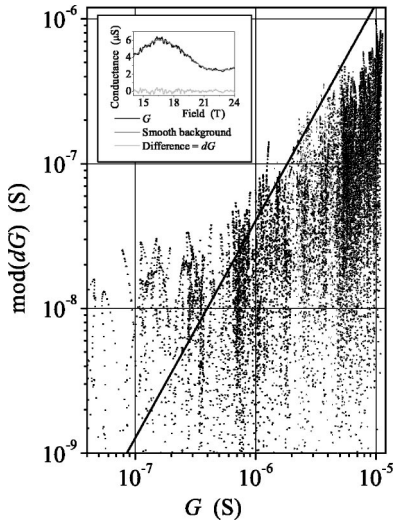
FIG. 10. Deviation of the conductance from a smooth background as a function of the conductance. The plot includes data from measurements with in-plane magnetic field. The different shapes represent different bars and different in-plane field. The solid line shows a dependence where dG is proportional to $G^{3/2}$ as described in Sec. V C. The inset illustrates how dG was obtained. A smooth curve is fitted to the raw data, and the difference is taken to be the fluctuations. The modulus of dG is taken to be the size of the deviation.

Figure 10 shows the size of the conductance fluctuations as a function of the absolute conductance. The magnitude of the deviation of the conductance from the smooth background is plotted against the conductance. Each point represents an average over a field range of ≈ 15 mT. The data includes all two-terminal bar samples, including data with in-plane magnetic field. All datasets show behavior consistent with the overall trend. The overall trend is that the size of the fluctuations increases monotonically with the conductance.

V. SIMPLE MODEL

Figure 11 (a(i)) shows a schematic diagram of the energies of the lowest electron and hole Landau levels as a function of position across the sample. For the electrons, close to the mesa edges, the confinement pushes the energies upwards, while the opposite is the case for the holes. Since the direction of the transport along the edge states is given by the gradient of $E(x)$ the electrons and holes contribute edge channels at the mesa edge with opposite directions.

We argue that in the insulating states, the transport properties of the mesa edges are determined by the behavior of the pairs of edge states. Their properties will depend strongly upon the way in which they interact, and the influence of disorder.

A. Edge channels and disorder

If there are no interactions at all, there will be no strongly resistive state when $\nu_e = \nu_h$ since this situation will be identical to one where two single-carrier-type Hall bars of oppo-
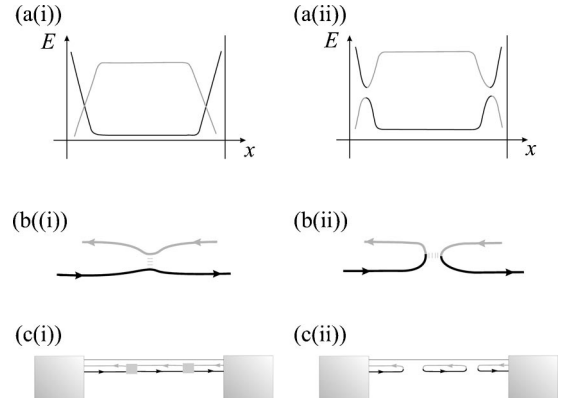

FIG. 11. (a(i)) Schematic diagram of the lowest electron and hole Landau levels as a function of position across a mesa. (a(ii)) is same as (a(i)) but with anticrossing behavior. (b) Diagrams showing edge channels. (b(i)) The interaction is weak, and the edge channels are not grossly affected. (b(ii)) Strong interaction leading to the formation of loops. (c(i)) A mesa edge with a series of junctions. (c(ii)) A mesa edge where the junctions are drawn as u turns.

site type are connected at each of their contacts.[15–17] The large resistance we measure is due to the electrons being allowed to move from one edge channel to another.

Figure 11 (a(i)) shows a schematic diagram of the Landau-level energies as a function of position across the mesa. One of each electron and hole Landau levels is occupied. Interactions between the electron and hole edge states will lead to the formation of an energy gap, where they would otherwise cross in energy. If the Fermi energy were to lie within the gap, there will be no edge states, and the system would be totally insulating. If instead the Fermi energy lies outside of the gap, there will be edge states as in the case of no interactions, and no high resistance behavior would be observed. Our experimental data shows that neither of these cases describes the full picture, as we always observe large but finite resistance.

Since the sample-to-sample variation in the resistance is strong, disorder must be playing a major role in determining the behavior. The effect of a disordered energy landscape on the edge states is that it changes the position of the electron and hole edge channels with respect to each another.

Interactions between the electron and hole edge channels will be favored when they are close together, and weaker when they are further apart. The disorder therefore determines the positions at which interactions can occur. We will refer to these positions or regions as "junctions."

The way in which these junctions should be pictured depends on the effect of the interactions on the states. If the junctions only represent points at which there is a small probability of an electron transferring from one channel to the other, they can be suitably depicted as shown in Fig. 11(b(i)). If the interactions are strong, the system may be better considered as depicted in Fig. 11(b(ii)) where the energy gap forces the edge channels to form u turns at the junctions, and therefore a series of loops along the mesa edge as shown in Fig. 11(c(ii)).

Experimentally, we have found that the conduction is Ohmic with respect to applied voltage, and has very weak
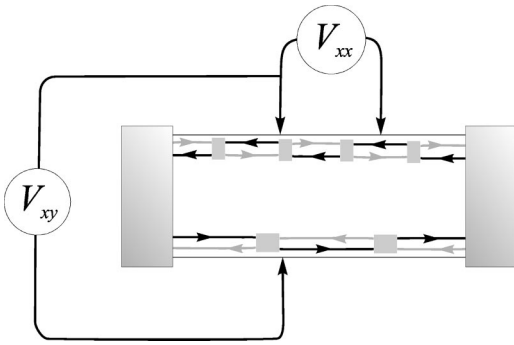
FIG. 12. Figure to show the global scenario in a Hall bar. The gray blocks represent ''Ohmic regions'' where the electron and hole edge channels interact, where the electrical potential is dropped and dissipation occurs. V_{xy} measured across symmetrically opposite voltage probes can measure a finite value leading to the symmetric Hall resistance.

FIG. 13. Top: A schematic diagram of a mesa edge when there are two edge channels contributed by both electrons and hole. l_s shows the length of a typical unit section. The lower diagram is a schematic illustrating how the size of the conductance fluctuations is calculated.

temperature dependence. This suggests that the junctions are behaving as Ohmic resistors with very weak temperature dependence. This shows that the system is not simply a series of usual localized states[18] as such systems are found to be strongly temperature dependent.[19–21] A previous theoretical study[22] has found that the limiting conductance of a disordered set of counterpropagating edge states is given by the net number of edge states in the majority direction (i.e., $\nu_h - \nu_e$). While this is consistent with the observation of compensated quantized Hall states[6] when $\nu_e \neq \nu_h$, it only predicts the limiting case of strong localization when $\nu_e = \nu_h$.

We have not been able to assign what microscopic mechanism is responsible for the behavior we observe, but these considerations show that inhomogeneous electron-hole channels can form along the mesa edge. Dissipation and voltage drops occur at the junctions where the electron and hole edge channels interact, leading to a highly inhomogeneous wire.

B. Global behavior

A schematic diagram of the resulting edges for a Hall bar is shown in Fig. 12. The gray blocks represent the interacting regions, or junctions behaving as Ohmic resistors. The energy and length scales associated with the inter-edge channel interactions and the disorder determine the resistance of these resistors.

Data from the series of bars where the length and width were varied showed that the sample-to-sample variations in the conductance are typically of over one order of magnitude, showing that the edge conduction is highly inhomogeneous even on the length scale of hundreds of micrometers. The distribution of the resistive junctions must also be inhomogeneous on this length scale.

The figure schematically shows differently arranged junctions on two sides of a bar. A measurement of the voltage across probes positioned symmetrically opposite each other will measure a finite voltage. The size of this voltage can be of the same order as the longitudinal voltage, if circumferential distances of the same order of magnitude separate the contacts.
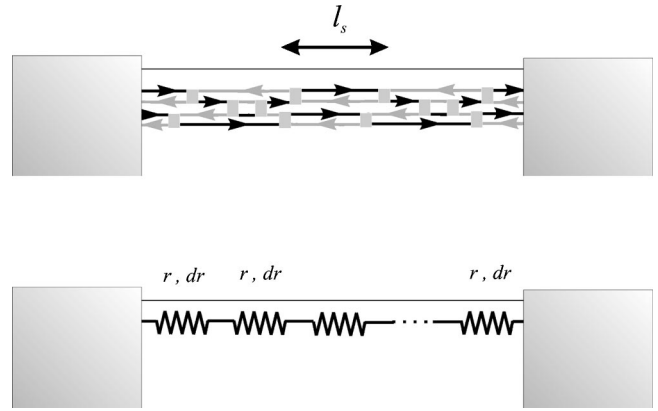
C. Fluctuations

We interpret the magnetoconductance fluctuations in terms of universal conductance fluctuations. In narrow wires over which there is phase coherence, it has been found that the conductance fluctuates by an amount of order e^2/h. For wires longer than the phase-coherence length l_ϕ, the fluctuations behave as expected for a chain of resistors,[23] each representing a section of length l_ϕ.

The inhomogeneity of our system suggests that l_ϕ may not be well defined. However, we can suppose that a section of length l_s may be defined, demarcated by junctions. Figure 13 shows a schematic diagram of a mesa edge where there are two pairs of edge channels. These will arise if $\nu_e - \nu_h = 2 - 2$. l_s represents the length of a ''typical'' unit section.

If the junction resistors behaved as perfect ideal Ohmic contacts, a section consisting of a pair of counterpropagating edge channels terminated by Ohmic contacts will have a resistance of h/e^2. If there are two pairs of edge channels the resistance of a section will be $h/2e^2$. If this was the case and the junctions behaved as ideal contacts, the inhomogeneity of the wire resistance will be entirely due to the inhomogeneity in the spatial distribution of the junctions. Even if this were not the case, it is conceivable that we can define a characteristic conductance g (or resistance $r = 1/g$) which has a representative value for all sections; g depending on the junction, not the length.

Now suppose that the conductance of each section fluctuates by an amount dg. The resistance of each section therefore fluctuates by dr:

$$dr = \frac{1}{g^2} dg. \tag{3}$$

The total resistance R of the wire is the sum of N individual sections:

$$R = N/G = Nr = 1/G, \tag{4}$$

where G is the conductance of the entire wire. The fluctuating part of the resistance performs a random walk so that the standard deviation of the resistance is

$$dR = N^{1/2}dr. \tag{5}$$

It follows then that the conductance of the entire chain G fluctuates by dG given by

$$dG = G^2 dR \tag{6}$$

$$\Rightarrow dG = \left(\frac{G}{g}\right)^{3/2} dg. \tag{7}$$

Figure 10 shows a solid line with this dependence with $g = 2e^2/h$ and $dg = e^2/h$. These values would be expected if a section were composed of two pairs of edge channels and each section contributed fluctuations equivalent to that from one phase-coherence length.

At large values of G, the agreement to the $dG \propto G^{3/2}$ law is reasonable, while at lower values below ~ 1 μS, the size of the fluctuations is underestimated. This suggests that when G is large, the assumption of a characteristic conductance g associated with each section is correct, and that the number of these sections varies strongly from sample to sample to give the observed sample-to-sample variation, as we have supposed. At lower values of G, the behavior deviates from this description which we interpret as being due the conductance per section g decreasing. This could be because as the number of sections increases, the likelihood of the sample containing exceptionally small values of individual g increases.

D. The background conductance and its behavior with field

When G, the total conductance of an edge, is large, it is determined by the number of sections there are along the edge. The number of sections is determined by how often the edge channels come into close proximity to each other.

Figure 14 illustrates how this is related to the extent to which these channels are delocalized across the sample due to disorder, which in turn would be expected to be related to the localization length. If the spatial extents of the electron and hole edge channels λ_e and λ_h are sufficiently small compared with their average separation d, points at which the two edge channels cross will be rare. As λ_e and λ_h increase the length between junctions will decrease, therefore increasing the number of sections. This will reduce the total conductance.

We interpret the smooth systematic background variation of the conductance with magnetic field to be due to this. All data shown in Fig. 6 show minima in conductance at the low- and high-field ends of the insulating state. As the field is increased or decreased from the center of the insulating state, the localization length increases leading to a larger number of sections, in turn leading to smaller conductance and smaller magnetoconductance fluctuations. This is confirmed by the conductance of the two-terminal bars in tilted magnetic field as shown in Fig. 9. As the in-plane field is increased, the conductance of the sample interior increases as
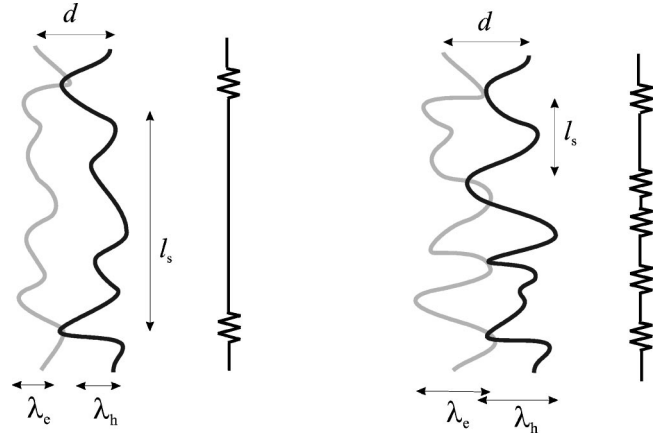

FIG. 14. Schematic diagrams illustrating the position of the electron and hole edge channels in the plane of the sample. λ_e and λ_h are the length scales of the meandering edge channels, related to their localization lengths. l_s is the length of a resultant section. The circuit diagrams represent the corresponding circuits, if a certain resistance is incurred at every junction.

the range in field of the insulating state narrows. The increase of the conductivity σ_{xx} corresponds to an increase in the localization length. The two-terminal bars show a corresponding opposite behavior, where the conductance decreases as the parallel field is applied. A larger localization length gives a smaller conductance.

VI. DISCUSSION

We have shown that the simple model based on edge states can be used to interpret the qualitative aspects of the observed behavior. In this section, we present some comments on two natural questions arising from the previous sections.

A. Surface potential at the mesa edge

If the electron-hole anticrossing is extremely strong and there are no electron-hole edge channels present at the mesa edges, might there be some other contribution of current carrying states at the mesa edges? Such states could be contributed due to the InAs having the Fermi energy pinned at an energy much higher than the conduction-band edge. The Fermi energy at the InAs surface is pinned above the conduction-band edge, by an amount 100–150 meV depending on the chemical preparation.[24,25] This effect is exploited in the study of nanostructures, including narrow wires showing magnetoconductance fluctuations.[26,27]

Consideration of how the Landau levels vary as they approach the edges shows, however, that although the surface pinning may introduce extra pairs of counterpropagating edge channels, the net number of edge channels in a given direction will always be governed by the quantized occupancy in the sample interior. These channels could not, however, account for the strongly correlated behavior between the edge conductance and the internal conductivity.

While we cannot rule out the possibility that such extra edge channels exist, the observation that the edges and the
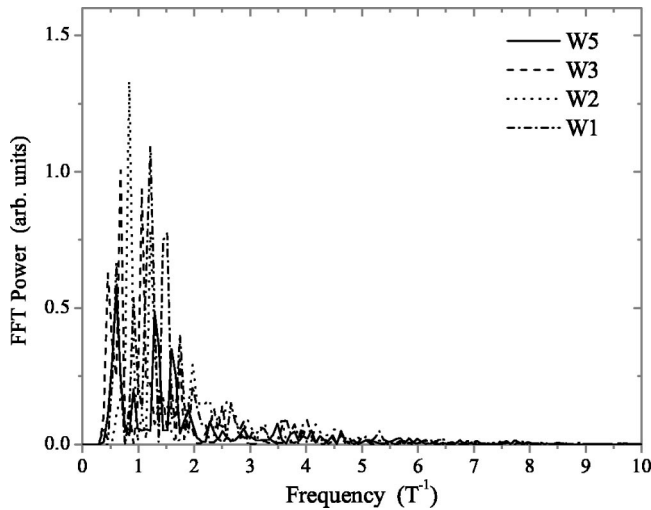
FIG. 15. Fourier transforms of the fluctuating part of the conductance between 14 and 23 T on the series of two-terminal bars where the width has been varied.

interior show opposite behavior with magnetic field strongly suggests that edge channels contributed by Landau levels occupied in the sample interior control the edge conduction in support of our model.

B. Field scale of the fluctuations

Assigning the conductance fluctuations to universal conductance fluctuations leads to the possibility of extracting a corresponding area scale.[28] The typical "period" in magnetic field ΔB is related to the typical area A enclosed by the interfering paths by

$$\Delta B = \frac{h}{eA}. \tag{8}$$

We have been unable to obtain systematic variations in the frequency distributions associated with the fluctuations. However, the field scale of the fluctuations seems to be relatively constant. Figure 15 shows the Fourier transforms of the fluctuating part of the conductance between 14 and 23 T on the series of bars where the width has been varied. The spectrum shows largest values between 0.5 and 2 T^{-1}. One limitation of the data is that areas much smaller than this could not be seen due to the way in which we have interpreted the smooth background. Features of field scale greater than about 2 T will be removed which will limit frequency spectrum below 0.5 T^{-1}.

The typical field scale in the data of the largest fluctuations is of order 1 T and this gives $A^{1/2} \sim 60$ nm. If the fluctuations were due to interference between electrons having traveled through different edge states, the area would correspond to the area of a section of length l_s. We do not consider this likely as the relationship between the size of the fluctuations and the conductance suggests that the conductance per section is of order of a few conductance quanta. The number of sections per sample would then be of order 100, so that the typical length of a section would be of order of a few micrometers or greater. Achieving an area $A^{1/2} \sim 60$ nm with this length scale requires widths of order Angstroms/nanometres. This seems somewhat unrealistic, considering that even the magnetic length $(h/eB)^{1/2}$ is as much as ~ 6 nm at 20 T. Instead, we speculate that the area corresponds to the size scale of the junctions.

It is possible that the width scale of the edge channels are such that the areas enclosed by their paths are too large to observe their corresponding interference effects with the experimental accuracy used. Alternatively, their circumferential extent may be longer than the phase-coherence length. Although some authors claim that the phase-coherence lengths of edge states are macroscopically large[29–31] (of the order of millimeters), measurements of interference effects showing oscillations with magnetic field seem to only occur over much more modest length scales of order micrometers[32] to tens of micrometers,[33] with the latter observed at 15 mK but not 50 mK.

VII. CONCLUSIONS

We have presented geometry dependent measurements and have shown that the conductance leading to the saturated longitudinal resistance and the symmetric Hall resistance occurs due to the mesa edges. A consideration of edge states in the system has shown how an inhomogeneous channel comprising electron and hole edge channels and their junctions can form at the mesa edge. We have presented a simple qualitative interpretation of the observed conductance, including the fluctuations, in terms of the edge channels.

ACKNOWLEDGMENTS

[1] R.J. Nicholas, K. Takashina, M. Lakrimi, B. Kardynal, S. Khym, N.J. Mason, D.M. Symons, D.K. Maude, and J.C. Portal, Phys. Rev. Lett. **85**, 2364 (2000).

[2] L. Esaki and L.L. Chang, J. Magn. Magn. Mater. **11**, 208 (1979).

[3] L.L. Chang, N. Kawai, G.A. Sai-Halasz, R. Ludeke, and L. Esaki, Appl. Phys. Lett. **35**, 939 (1980).

[4] M. Alterelli, J.C. Maan, L.L. Chang, and L. Esaki, Phys. Rev. B **35**, 9867 (1987).

[5] S. Holmes, W.T. Yuen, T. Malik, S.J. Chung, A.G. Norman, R.A. Stradling, J.J. Harris, D.K. Maude, J.C. Maude, and J.C. Portal, J. Phys. Chem. Solids. **56**, 445 (1995).

[6] E.E. Mendez, L. Esaki, and L.L. Chang, Phys. Rev. Lett. **55**, 2216

(1985).

[7] M.S. Daly, K.S.H. Dalton, M. Lakrimi, N.J. Mason, R.J. Nicholas, M. van der Burgt, P.J. Walker, D.K. Maude, and J.C. Portal, Phys. Rev. B **53**, R10 524 (1996).

[8] B.I. Halperin, Phys. Rev. B **25**, 2185 (1982).

[9] N.J. Mason in *Atomic Layer Epitaxy*, edited by T. Suntola and M. Simpson (Blackie, London, 1990).

[10] N.J. Mason and P.J. Walker, J. Cryst. Growth **108**, 181 (1991).

[11] L. Onsager, Phys. Rev. **38**, 2265 (1931).

[12] G. Nachtwei, Physica E (Amsterdam) **4**, 79 (1999).

[13] J.C. Licini, D.J. Bishop, M.A. Kastner, and J. Melngailis, Phys. Rev. Lett. **55**, 2987 (1985).

[14] P.A. Lee, A.D. Stone, and H. Fukuyama, Phys. Rev. B **35**, 1039 (1987).

[15] F.F. Fang and P.J. Stiles, Phys. Rev. B **29**, 3749 (1984).

[16] F.F. Fang and P.J. Stiles, Phys. Rev. B **27**, 6487 (1983).

[17] M. Buttiker, Phys. Rev. B **38**, 9375 (1988).

[18] P.W. Anderson, Phys. Rev. **109**, 1492 (1958).

[19] P. Lee, Phys. Rev. Lett. **53**, 2042 (1984).

[20] J. KurkiJarvi, Phys. Rev. B **8**, 922 (1973).

[21] R.A. Serota, R.K. Kalia, and P.A. Lee, Phys. Rev. B **33**, 8441 (1986).

[22] C. Barnes, B.L. Johnson, and G. Kirczenow, Phys. Rev. Lett. **70**, 1159 (1993).

[23] Y. Imry, *Introduction to Mesoscopic Physics* (Oxford University Press, New York, 1997).

[24] S. Kawaji and H.C. Gatos, Surf. Sci. **7**, 215 (1967).

[25] D.C. Tsui, Phys. Rev. Lett. **24**, 303 (1970).

[26] R.J. Haug, H. Munetaka, and L.L. Chang, Jpn. J. Appl. Phys., Part 1 **31**, 127 (1992).

[27] F. Stern and S.E. Laux, J. Appl. Phys. **72**, 809 (1992).

[28] Y. Aharanov and D. Bohm, Phys. Rev. **115**, 485 (1959).

[29] T. Machida, H. Hirai, S. Komiyama, and Y. Shiraki, Physica B **249-251**, 128 (1998).

[30] T. Machida, H. Hirai, S. Komiyama, and Y. Shiraki, Phys. Rev. B **54**, 16 860 (1996).

[31] See comments in J.J. Lin and J.P. Bird, J. Phys.: Condens. Matter **14**, R501 (2002).

[32] J. Liu, W.X. Gao, K. Ismail, K.Y. Lee, J.M. Hong, and S. Washburn, Phys. Rev. B **50**, 17 383 (1994).

[33] Y. Ji, Y.C. Chung, D. Sprinzak, M. Heiblum, D. Mahalu, and H. Shtrikman, in *Physics of Semiconductors 2002*, Institute of Physics Conference Series 171, edited by A.R. Long (Institute of Physics, London, 2003).